Microelectronic Engineering 98 (2012) 409–413

Contents lists available at SciVerse ScienceDirect

Microelectronic Engineering

journal homepage: www.elsevier.com/locate/mee

Controllable three dimensional deformation of platinum nanopillars by focused-ion-beam irradiation

Ajuan Cui, Wuxia Li *, Qiang Luo, Zhe Liu, Changzhi Gu *

Beijing National Laboratory for Condensed Matter Physics, Institute of Physics, Chinese Academy of Sciences, Beijing 100190, China

ARTICLE INFO

Article history:
Available online 7 June 2012

Keywords:
Focused-ion-beam
Freestanding
Platinum nanopillar
Controllable deformation

ABSTRACT

Freestanding nanostructures are fundamental elements to construct three-dimensional (3D) nanodevices. The bending of nanopillars by ion irradiation can be used to produce overhanging nanostructures. In this paper, we report the bending of focused-ion-beam (FIB) grown platinum nanopillars by FIB irradiation. The results show that for nanopillars originally perpendicular to the substrate, by adjusting the relative geometry of the incident ion beam and the nanopillars, desired bending direction and shape can be achieved. Such nanostructures can be used for 3D nanodevice constructions. Besides, ion irradiation with optimized conditions can be used to improve the surface morphology of the as-deposited nanopillars. Our results suggest that the method of bending freestanding nanoobjects using FIB is likely to be advantageous to construct interconnects in 3D nanostructures towards the properties investigations of selected individual nanoobjects.

1. Introduction

In recent years, technologies for 3D nanostructures fabrication have attracted intensive attention and several methods have been developed, including the FIB induced chemical vapor deposition (FIB-CVD) [1–5], nanoimprinting [6], laser fabrication [7], 3D photolithography [8], electron beam lithography and so on [9]. Among them, with the help of pattern-generating system, FIB-CVD has been demonstrated to be the most powerful 3D nanofabrication technique, which is capable of produce 3D asymmetric, overhanging, and hollow structures [1–5]. However, the direct writing of 3D nanostructures with a slowly moving ion beam requires sophisticated software packages and an expensive sample stage; it is time consuming to the point that structures can only be formed one-by-one and residual deposition underneath the suspended portion cannot be avoided; what's more, due to the stray dose and the beam-matter interactions during the growth process, it is very difficult to obtain 3D structures that are uniform in size by this method.

Most recently, a free-standing superconducting quantum interference device has been constructed using tungsten nanostructure grown by FIB-CVD, in the purpose of measuring magnetic field in both perpendicular and parallel directions [10]. However, the device performance was limited by the size variation along the wire edge and the residual deposition underneath the overhanging nanostructure. In order to produce surface clean 3D nanostructures with uniform size, a method based on the phenomenon of ion beam induced plastic-deformation has emerged. Bending of nanopillars or cantilevers including carbon nanotube [11], carbon nanopillars [12], and GaAs nanowires [13] have been reported. Until now, the bending of FIB-grown Pt nanopillars is to be reported though FIB-CVD grown lateral nanowires/strips that lying on the substrate surface have been widely used to form electrodes on nanowires/nanotubes. The reason of choosing FIB-grown freestanding Pt nanopillars as the targets of study lies in that FIB-CVD is a site-specific nanofabrication technique, and using this method, free-standing nanoobjects can be grown with good controllability in feature size, geometry and position, which could provide great flexibility in 3D nanodevices fabrication.

In order to build up a technology to form overhanging structures based on FIB-grown Pt nanopillars, the general bending effect under FIB irradiation was investigated. The ion beam current, the incident angle and the viewing magnification during ion irradiation have been explored in details to control the bending process.

2. Experimental details

All experiments were conducted in a dual-beam system with a gallium FIB (Strata DB-235, FEI) placed at an angle of 52° to the vertically oriented electron beam column. Pt nanopillars used in this study were grown on Al and Si substrates by FIB-CVD using a 1 pA ion beam current with $(CH_3)_3Pt$ ($CpCH_3$) as the precursor. For nanopillar deposition, first, the gas precursor molecules were

* Corresponding authors. Tel.: +86 10 82649098; fax: +86 10 82648198 (W. Li), tel.: +86 10 82648197; fax: +86 10 82648198 (C. Gu).
E-mail addresses: liwuxia@aphy.iphy.ac.cn (W. Li), czgu@aphy.iphy.ac.cn (C. Gu).

0167-9317/$ - see front matter © 2012 Elsevier B.V. All rights reserved.
http://dx.doi.org/10.1016/j.mee.2012.04.027

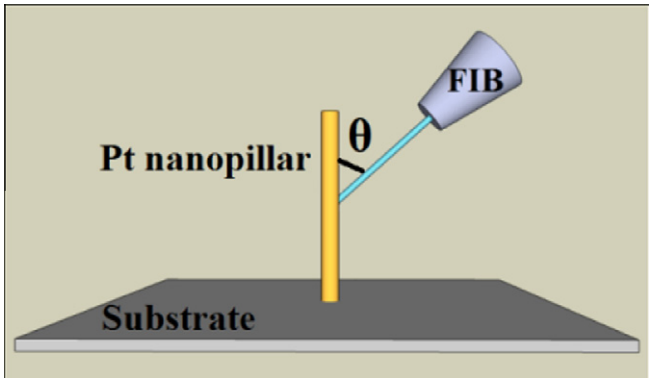

Fig. 1. The schematic diagram of the definition of the incident angle (θ): the angle between the ion beam and the as-deposited Pt nanopillar.

introduced to the substrate surface through a gas nozzle, and then a FIB with a nominal diameter of 7 nm was kept stationary in a particular position; this beam-scanning strategy was called spot-mode. The background pressure was about $5.5 \times 10^{-5} - 1.0 \times 10^{-6}$ mbar during deposition. The as-deposited Pt nanopillars were perpendicular to the substrate. The lengths and diameters of nanopillars used in this study lie in the range of 0.8–5 μm, and 130–330 nm, respectively.

To perform FIB-induced plastic-deformation of nanopillars, raster scanning was utilized to irradiate the whole field of view containing a nanopillar or a group of pillars. Throughout the process, the accelerating voltage of the Ga ions was set to 30 kV. The ion beam incident angle (θ), defined to be the angle between the incident ion beam and the long axis of the pillar as illustrated in Fig. 1, was varied by stage tilting since the ion beam incident direction is fixed. After each irradiation sweep, the stage was tilted to 45° off normal to the electron beam for bending measurement by in situ SEM imaging.

3. Result and discussion

First, the general bending effect was investigated using an ion beam current of 30 pA, an ion beam incident angle of 30° and a

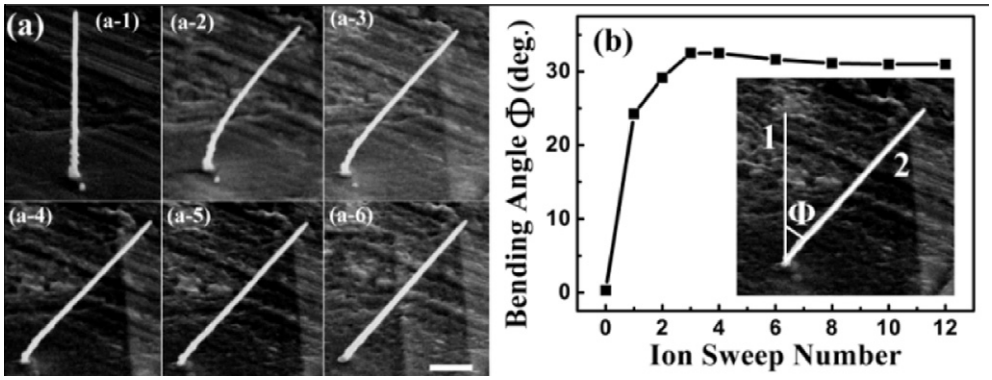

Fig. 2. (a) SEM images of the as-deposited Pt nanopillars (a-1) and that irradiated with an increasing of Ga ion-beam sweep number, showing the bending sequence (a-2)–(a-6). The scale bar is 1 μm and (b) The bending angle as a function of ion sweep number for FIB-grown Pt nanopillars, the inset was the definition of the bending angle (Φ), 1 and 2 for the orientations of the original and the bent nanopillar, respectively.

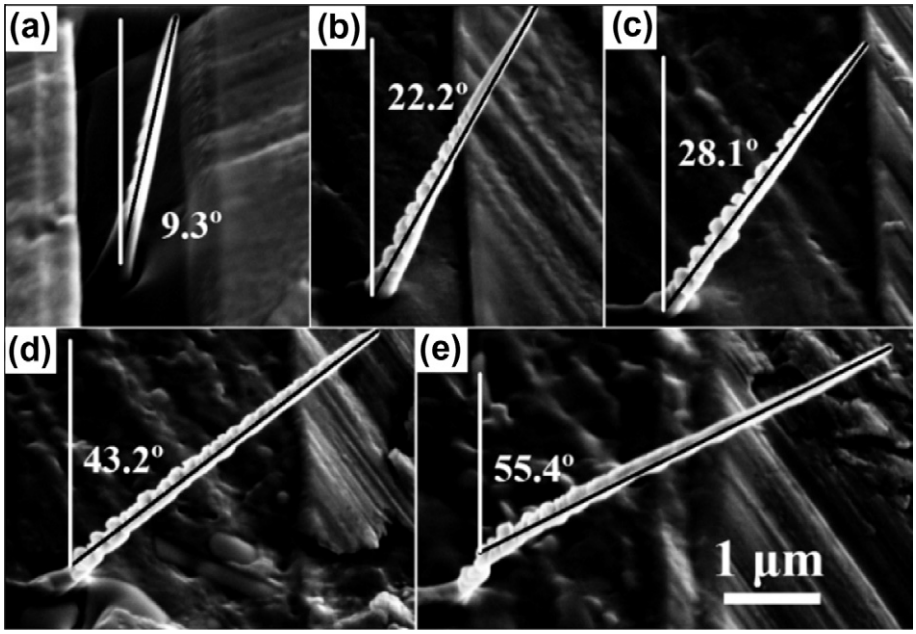

Fig. 3. The SEM images of the nanopillars aligned with the incident ion beam after being irradiated with ion beam incident angle of 10° , 20°, 30°, 40° and 50° for (a–e) respectively, the actual bending angles of the nanopillars were labeled in the images.

viewing magnification of 25,000. One ion sweep took 163s, which provided an ion dose of about 2.44×10^{13} ions/cm^2, thus the number of ions received by the nanopillar during the first sweep was about 1.55×10^8. The SEM images of Pt nanopillars irradiated with various ion beam sweep numbers are shown in Fig. 2a. The bending angle as a function of the ion sweep number is shown in Fig. 2b, the inset is the definition of the bending angle – the angle between the length direction of the original and the bent nanopillar. It can be seen from Fig. 2 that the nanopillar bent towards the incident ion beam with the bending angle increases with the ion sweep number until it becomes parallel to the incident beam, which indicates that the ultimate bending angle is determined by the ion beam incident angle. In order to confirm such observation, different incident angles, 10°, 20°, 30°, 40° and 50° were used; the resulted SEM images are showed in Fig. 3, in which the actual bending angles, 9.3°, 22.2°, 28.1°,43.2°, 55.4° are labeled correspondingly. Obviously, by adjusting the relative orientation of the pillars and the incident ion beam, the orientation of bent pillars can be precisely controlled; also, it can be judged from these data that the bending speed increases with increasing the incident angle under otherwise identical conditions.

In order to find out the influence of the nanopillar aspect ratio on the bending behavior, Pt nanopillars with aspect ratio of 3.55, 5.22, 6.65 and 22.20 (245 nm in diameter), were deposited. These nanopillars were then irradiated with identical condition using an ion beam current of 140 pA, an ion beam incident angle of 40° and a viewing magnification of 10,000. One ion sweep took 163s. The related ion dose was 1.80×10^{13} ions/cm^2 and the number of ions received during the first scan was 2.9×10^7, 4.4×10^7, 5.5×10^7, 1.84×10^8 for nanopillars with aspect ratio of 3.55, 5.22, 6.65 and 22.20, respectively. The bending angle of nanopillars with different aspect ratios as a function of the ion sweep number is shown in Fig. 4a and the corresponding SEM images monitoring the bending process is shown in Fig. 4b. It can be seen that at the initial stage, nanopillar with higher aspect ratio bent slightly faster though the time required for nanopillars with aspect ratio ranging from 3.55 to 22.20 to align with the incident ion beam is more or less the same.

We also found that during the bending process, the surface morphology can be modified by either performing prolonged ion irradiation using medium ion beam current (e.g. 30 pA) or using higher ion beam current (e.g. 100 pA) with a shorter exposure duration. As can be seen from Fig. 2a that after a number of ion sweeps with a 30 pA ion beam current, the pillar became smoother. For comparison, Pt nanopillars were also irradiated with a 100 pA ion beam current under magnification of 50,000 with an oblique incident angle of 30°. One ion sweep took 163s and the corresponding ion dose was of 3.21×10^{13} ions/cm^2. After one such scanning, the nanopillar bent to align with the incident ion beam. However, as can be seen from Fig. 5b as a comparison to Fig. 5a, the top section that facing the incident ion beam underwent obvious milling; it can also be seen that the surface roughness on that side has been improved significantly. Thus, by using proper ion beam current/ion dose, the surface morphology of freestanding nanoobjects can be modified during bending.

Meanwhile, the field of view, which can be easily changed by the viewing magnification, was also used to explore the effect of the ion dose on the bending process. The SEM images of three Pt nanopillars irradiated with viewing magnification of 15,000, 25,000 and 35,000 for pillar a, b and c under otherwise identical conditions are shown in Fig.6. In details, Fig. 6(a-2), (b-2) and (c-2) shows the images of pillars being irradiated with ion beam current of 50 pA and ion beam incident angle of 40°; Fig. 6(a-3), (b-3) and (c-3) shows the images of those after another irradiation sweep with ion beam current of 100 pA, and ion beam incident angle of 40°. With a 50 pA ion beam current, the ion dose was

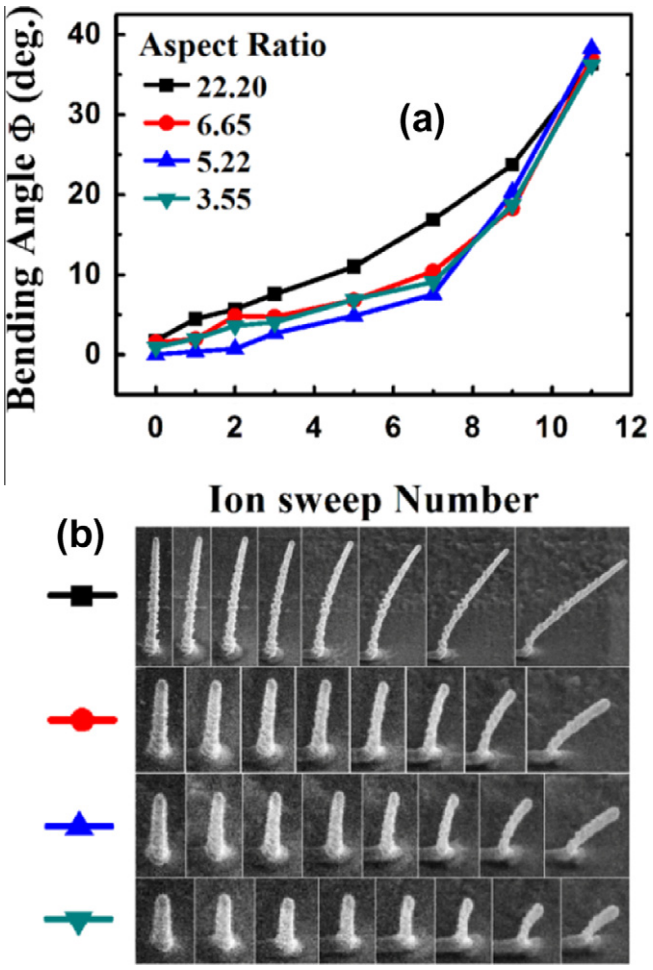

Fig. 4. The bending process of Pt nanopillars with various aspect ratios: (a) The bending angle as a function of ion sweep number for FIB-grown Pt nanopillars with aspect ratio of 3.55, 5.22, 6.65 and 22.20 and (b) the related SEM images showing the bending sequence.

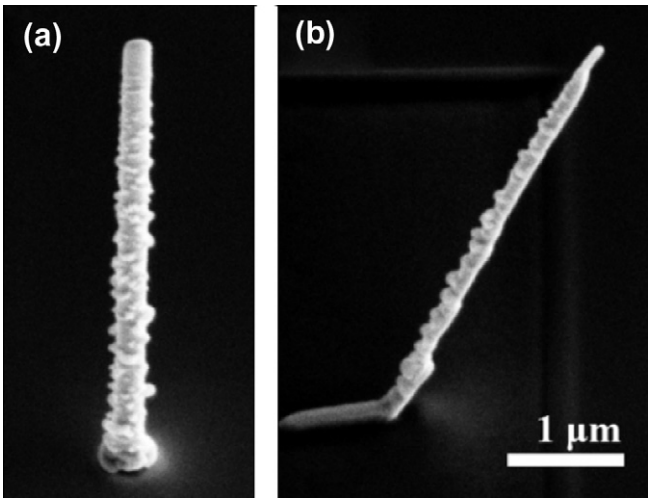

Fig. 5. The SEM images of the Pt nanopillars before (a) and after (b) FIB irridiation by a 100 pA ion beam current with ion beam incident angle of 30°. The viewing magnification during ion irradiation was 50, 000 and one ion sweep took 163s. The scale bar is 1 μm.

1.45×10^{13} ions/cm^2, 4.06×10^{13} ions/cm^2 and 7.89×10^{13} ions/cm^2 for the viewing magnification of 15,000, 25,000 and 35,000,

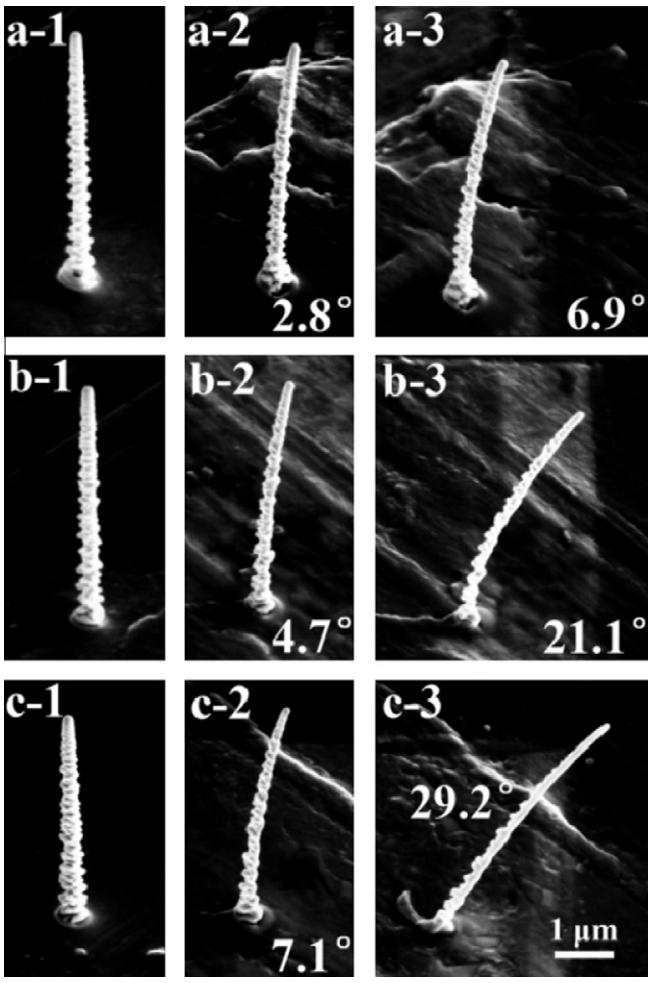

Fig. 6. The SEM images of Pt nanopillars a, b and c before (a-1, b-1, c-1) and after FIB irridiation with ion beam currents of 50 pA (a-2, b-2, c-2) and 100 pA (a-3, b-3, c-3), the ion beam incident angle is 40° and the magnification was 15,000, 25,000 and 35,000 for a, b, and c, respectively. The scale bar is 1 μm.

respectively; and the corresponding number of ions received by the nanopillars during the first sweep was 1.54×10^8, 4.51×10^8 and 7.75×10^8. It can be derived that the bending angle is not linearly proportional to the ion dose received by the pillars; however, it tells that the bending angle increases with increasing of the magnification before the nanopillar aligns with the incident ion beam. This is because the higher the magnification used during irradiation, the smaller the field of view, which resulted in a larger effective ion dose on the nanopillar. From above observations, we conclude that the ion beam current, ion beam incident angle and the viewing magnification (field of view) are factors that can be used to adjust the ion dose effectively, which then can be used to control the bending process of freestanding nanoobjects with reasonably good spatial precision.

The mechanisms of ion beam induced bending have been explored and discussed previously [12,14,15]. Arora et al. reported that the bending of micro-cantilevers of silicon nitride was due to the large compressive stresses generated by helium implantation [14]. However, Tripathi et al. reported a different phenomenon by performing Ga+ irradiation at the base of the carbon nanopillars and found that the base becomes thinner due to ion milling and eventually the structure collapses without Ga bubble formation [12]; accordingly, mechanism of temperature gradient induced bending of FIB-grown carbon nanopillars (with a negative thermal expansion coefficient) towards the incident ion beam was proposed by them [12]. Amorphized Ge nanowires were also found bent towards the ion beam, which could be well explained in terms of the viscoelastic thermal spike model for amorphous solids if their amorphized Ge nanowire persists a negative thermal expansion coefficient [15], which is yet to be confirmed. We observed a similar bending towards the incident ion beam for FIB-grown platinum nanopillars on Si and Al substrates. It has been reported that FIB-CVD Pt is amorphous and contains a large amount of carbon [16], which is very likely persists a negative thermal expansion coefficient. However, questions such as whether the bending towards the ion beam direction is mainly governed by the temperature gradient or by the strain generated during irradiation, or by the decomposing of residual gas molecules imbedded into one side of the pillar during post-growth irradiation, needed to be resolved? To answer such questions, further experiment for in-depth understanding of the bending mechanism is on the way.

4. Conclusion

In summary, we have developed a technique of site-specific shape manipulation of conducting Pt nanopillars by FIB irradiation induced plastic-deformation. Using ion dose in the range of 1.4×10^{13}–3.2×10^{14} ions/cm^2, the general bending trends have been investigated. In particular, Pt nanopillars were found to bend towards the incident ion beam until the wires become parallel to it, and then the bending angle saturates upon further irradiation. Parameters such as ion current, ion incident angle, ion beam sweep number and the viewing magnification can be used to control the bending process. Moreover, different ion dose could be used to achieve different surface morphologies of freestanding nanoobjects during bending. Thus we propose that FIB irradiation induced bending is likely to be advantageous to construct interconnects in 3D nanostructures towards the properties investigations of selected individual nanoobjects as well as to construct 3D nanodevices with novel properties.

Acknowledgments

This work is supported by National Natural Science Foundation of China under Grant Nos. 91123004, 11104334, 50825206, 10834012, and 60801043; and the National Basic Research Program (973) of China under Grant No. 2009CB930502, Chinese Service Center for Scholar Exchange, and Outstanding Technical Talent Program of the Chinese Academy of Sciences.

References

[1] T. Morita, R. Kometani, K. Watanabe, K. Kanda, Y. Haruyama, T. Hoshino, K. Kondo, T. Kaito, T. Ichihashi, J-i. Fujita, M. Ishida, Y. Ochiai, T. Tajima, S. Matsui, J. Vac. Sci. Technol. B 21 (2003) 2737–2741.
[2] T. Morita, K-i. Nakamatsu, K. Kanda, Y. Haruyama, K. Kondo, T. Hoshino, T. Kaito, J-i. Fujita, T. Ichihashi, M. Ishida, Y. Ochiai, T. Tajima, S. Matsui, J. Vac. Sci. Technol. B 22 (2004) 3137–3142.
[3] T. Bret, I. Utke, C. Gaillard, P. Hoffmann, J. Vac. Sci. Technol. B 22 (2004) 2504–2510.
[4] T. Hoshino, M. Kawamori, T. Suzuki, S. Matsui, K. Mabuchi, J. Vac. Sci. Technol. B 22 (2004) 3158–3162.
[5] T. Morita, K. Watanabe, R. Kometani, K. Kanda, Y. Haruyama, T. Kaito, J-i. Fujita, M. Ishida, Y. Ochiai, T. Tajima, S. Matsui, Jpn. J. Appl. Phys. 42 (2003) 3874–3876.
[6] K. Watanabe, T. Morita, R. Kometani, T. Hoshino, K. Kondo, K. Kanda, Y. Haruyama, T. Kaito, J. Fujita, M. Ishida, Y. Ochiai, T. Tajima, S. Matsui, J. Vac. Sci. Technol. B. 22 (2004) 22–26.
[7] A.I. Kuznetsov, R. Kiyan, B.N. Chichkov, Opt. Express. 18 (2011) 21199.
[8] L-j. Li, R. G, J. Fourkas, SPIE Newsroom 24 (2009) 1690.
[9] V. Kudryashov, X.C. Yuan, W.C. Cheong, K. Radhakrishnan, Microelectron. Eng. 67–68 (2003) 306–311.
[10] E.J. Romans, E.J. Osley, L. Young, P.A. Warburton, W. Li, Appl. Phys. Lett. 97 (2010) 222506.
[11] B.C. Park, K.Y. Jung, S.J. Ahn, J. Choi, D-H. Kim, J. J. Appl. Phys. 45 (2006) L1162–L1164.

[12] S.K. Tripathi, N. Shukla, S. Dhamodaran, V.N. Kulkarni, Nanotechnology 19 (2008) 205302.
[13] C. Borschel, R. Niepelt, S. Geburt, C. Gutsche, I. Regolin, W. Prost, F.-J. Tegude, D. Stichtenoth, D. Schwen, C. Ronning, Small 5 (2009) 2576–2580.
[14] W.J. Arora, S. Sijbrandij, L. Stern, J. Notte, H.I. Smith, G. Barbastathis, J. Vac. Sci. Technol. B. 25 (2007) 2184–2187.
[15] L. Romano, N.G. Rudawski, M.R. Holzworth, K.S. Jones, S.G. Choi, S.T. Picraux, J. Appl. Phys. 106 (2009) 114316.
[16] J.-F. Lin, J.P. Bird, L. Rotkina, A. Sergeev, V. Mitin, Appl. Phys. Lett. 84 (2004) 3828.